

# Query-Free Black-Box Adversarial Attacks on Graphs

Jiarong Xu  
Zhejiang University  
xujr@zju.edu.cn

Yizhou Sun  
University of California, Los Angeles  
yzsun@cs.ucla.edu

Xin Jiang  
University of California, Los Angeles  
jiangxjames@ucla.edu

Yanhao Wang  
Zhejiang University  
wangyanhao@zju.edu.cn

Yang Yang  
Zhejiang University  
yangya@zju.edu.cn

Chunping Wang  
FinVolution Group  
wangchunping02@xinye.com

Jiangang Lu  
Zhejiang University  
lujg@zju.edu.cn

## ABSTRACT

Many graph-based machine learning models are known to be vulnerable to adversarial attacks, where even limited perturbations on input data can result in dramatic performance deterioration. Most existing works focus on moderate settings in which the attacker is either aware of the model structure and parameters (white-box), or able to send queries to fetch model information. In this paper, we propose a query-free black-box adversarial attack on graphs, in which the attacker has no knowledge of the target model and no query access to the model. With the mere observation of the graph topology, the proposed attack strategy flips a limited number of links to mislead the graph models. We prove that the impact of the flipped links on the target model can be quantified by spectral changes, and thus be approximated using the eigenvalue perturbation theory. Accordingly, we model the proposed attack strategy as an optimization problem, and adopt a greedy algorithm to select the links to be flipped. Due to its simplicity and scalability, the proposed model is not only generic in various graph-based models, but can be easily extended when different knowledge levels are accessible as well. Extensive experiments demonstrate the effectiveness and efficiency of the proposed model on various downstream tasks, as well as several different graph-based learning models.

## CCS CONCEPTS

• **Computer systems organization** → **Embedded systems**; *Redundancy*; Robotics; • **Networks** → Network reliability.

## KEYWORDS

adversarial attack, graph learning, eigenvalue perturbation theory

## ACM Reference Format:

Jiarong Xu, Yizhou Sun, Xin Jiang, Yanhao Wang, Yang Yang, Chunping Wang, and Jiangang Lu. 2018. Query-Free Black-Box Adversarial Attacks

Permission to make digital or hard copies of all or part of this work for personal or classroom use is granted without fee provided that copies are not made or distributed for profit or commercial advantage and that copies bear this notice and the full citation on the first page. Copyrights for components of this work owned by others than ACM must be honored. Abstracting with credit is permitted. To copy otherwise, or republish, to post on servers or to redistribute to lists, requires prior specific permission and/or a fee. Request permissions from [permissions@acm.org](mailto:permissions@acm.org).  
Conference'17, July 2017, Washington, DC, USA

© 2018 Association for Computing Machinery.  
ACM ISBN 978-x-xxxx-xxxx-x/YY/MM... \$15.00  
<https://doi.org/10.1145/1122445.1122456>

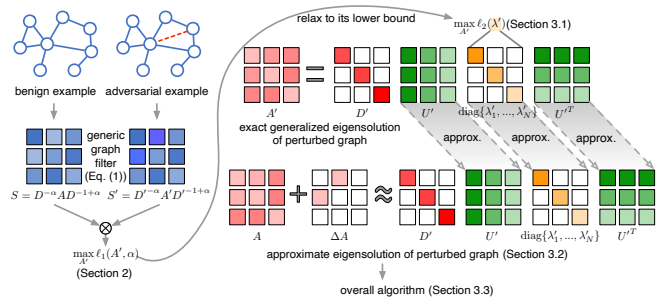


Figure 1: Overview of query-free black-box adversarial attacks on graphs.

on Graphs. In *Proceedings of ACM Conference (Conference'17)*. ACM, New York, NY, USA, 13 pages. <https://doi.org/10.1145/1122445.1122456>

## 1 INTRODUCTION

Deep learning on graphs has achieved significant success in a large number of applications [14], including molecule analysis [16], drug discovery [13], financial surveillance [26] and recommendation systems [32], *etc.* However, these approaches have been shown to be vulnerable to adversarial examples [3, 8, 11, 44], namely those that are intentionally crafted to fool the models through slight, even human-imperceptible modifications to benign examples. Therefore, adversarial attack presents itself as a serious security challenge for many real-world systems, and is of great importance to identify the weaknesses of these graph learning models.

Many efforts have been devoted to studying adversarial attack strategies on graphs. As the first attempt, white-box attacks, assume full access to the target (a.k.a. the victim model), including the model structure and the learned parameters. Thus, many gradient-based algorithms have been proposed to generate adversarial examples under white-box attack settings [7, 33, 36, 37]. However, it is often unrealistic to assume an attacker will have complete knowledge of a learning model. Gray-box attacks are proposed under such consideration where the attackers usually train surrogate models with the task-specific labeled data and take advantage of their information to approximate the victim ones [19, 43, 44]. Whereas, as many graphs in the wild are unlabeled and it is arduously expensive to obtain sufficient labels, which motivates the study of black-box attacks. In most black-box settings, the target model and training

labels are unknown to adversaries, but it is possible to query some or all of the examples and utilize the outputs from a victim model [11, 39]. Unfortunately, in most real-world scenarios, the attacker’s potential attempt like querying the target model is more likely to be noticed or even can not bypass the defenders. In addition, these queries are either costly in terms of money and time or prohibited due to security reasons, copyright issues, *etc.* For example, a credit risk model built upon an online payment network is hidden behind company API wrappers, and thus inaccessible to the public. In this case, no query access is available, and so attacks towards this model should be not only black-box but query-free as well.

In this paper, we target a more challenging setting and propose a query-free black-box attack strategy on graphs (Cf. Figure 1 for an overview). In literatures, the attackers can generate graph adversarial perturbations by manipulating the graph structure or node attributes to fool the target models. In our case, we assume the attacker operates on plain graph structure.

Given the graph structure, our studied question is: *Which set of edges has the most significant influence on the graph?* A straightforward approach is to capture the impact of edge flips by the spectral change of the adjacency matrix, because spectrum can reflect many graph intrinsic properties (*e.g.*, graph connectivity). However, the spectrum of different perturbed adjacency matrices is not bounded in a same range [9]. This makes the spectrum of the original and perturbed adjacency matrix less comparable (see the analysis of objective function part in § 4.2 for details). Since the black-box attacker has no knowledge about the target model, we therefore propose to capture the perturbation impact by the change in a generic graph filter which is applicable to various graph models (§ 2). Furthermore, we will show latter that the spectrum of the graph filter preserves across most graph models and is bounded in  $[-1, 1]$ . The adversarial attack then can be modeled as a constrained optimization problem associated with the graph filter under certain perturbation budget, which is a non-convex optimization problem. We analyze and relax the problem to optimize the objective’s lower bound, which is convex and only involves with the spectrum of graph filter, but not the associated eigenvectors. However, re-evaluating the spectrum of every possible set of perturbed spectrum is computationally expensive. In order to efficiently compute the slight change in the graph spectrum, we adopt the eigenvalue perturbation theory to approximate the perturbed spectrum. Thereby, the relaxed optimization problem can be easily solved using a greedy algorithm, resulting in a clever choice of edge sets with a significant impact on the graph filter. Furthermore, the proposed attack strategy is not only generic for attacking a number of graph-based learning models, but can also be easily extended to different knowledge levels to boost the performance of many existing attackers.

We summarize our contributions as follows:

- We target a critical yet overlooked query-free black-box adversarial attack on graphs.
- We propose a generic graph filter which is applicable to various graph models.
- We develop an efficient attack strategy to select adversarial edges via eigenvalue approximation theory.
- Numerical experiments demonstrate the effectiveness of the relaxation and the scalability of the attack model.

## 2 PROBLEM DEFINITION

Let  $G = (V, E)$  be an undirected and unweighted graph with the node set  $V = \{v_1, v_2, \dots, v_N\}$  and the edge set  $E \subseteq V \times V$ . The adjacency matrix  $A$  of the graph  $G$  is an  $N \times N$  symmetric matrix with elements  $A_{ij} = 1$  if  $\{i, j\} \in E$  or  $i = j$ , and  $A_{ij} = 0$  otherwise. Note that we set the diagonal elements of  $A$  as 1 to allow for self-loops. The degree matrix  $D$  is an  $N \times N$  diagonal matrix with diagonal elements denoting the node degrees, *i.e.*,  $D_{ii} = \sum_{j=1}^N A_{ij}$ .

**Generic graph filter.** We define a generic graph filter  $S$  as a function of  $A$ , *i.e.*,

$$S = D^{-\alpha} A D^{-1+\alpha}, \quad (1)$$

where  $\alpha \in [0, 1]$  is a given parameter.

- **Connection to existing graph models:** Many common choices of graph filters can be considered as special cases of the generic graph filter  $S$ . For instance, when  $\alpha = 1/2$ , the corresponding graph filter  $S_{\text{sym}} = D^{-1/2} A D^{-1/2}$  is symmetric, and used in various applications, including spectral graph theory [9] and the graph convolutional networks [20, 25, 35]. Another common choice of  $\alpha$  is  $\alpha = 1$ , and the resulting graph filter  $S_{\text{rw}} = D^{-1} A$  is widely used in many applications related to random walks on graphs [9]. It is well known that many graph properties can also be expressed in terms of the graph filter  $S_{\text{rw}}$  [24]. Furthermore, it is easy to see the connection between the graph filter and the graph Laplacian ( $L = D - A$ ), *i.e.*,  $S = I - D^{-\alpha} L D^{-1+\alpha}$ , where the change in  $S$  and the change in  $D^{-\alpha} L D^{-1+\alpha}$  is exactly the same.
- **Property:** One property of the generic graph filter  $S$  is the invariance of spectrum under  $\alpha$ , *i.e.*, its intrinsic spectral properties (*e.g.*, distances between vertices, graph cuts, the stationary distributions of a Markov chain [10, 29]) are preserved regardless of the choice of  $\alpha$ .

**Query-free black-box adversarial attack on graphs.** In this work, we assume that the adversarial attacker can add or delete a limited number of edges from  $G$ , resulting in a perturbed graph  $G' = (V, E')$ . We target on a critical yet far overlooked query-free black-box attack, in which the attacker has no knowledge about the victim model and is unable to query any examples, but can only observe the input graph. Without the access to any information from models and queries, we accordingly aim to capture the changes to graph filter  $S$  caused by the graph adversarial attack. This convention is adopted by most graph learning models, because one edge flip  $\{i, j\}$  in the graph filter  $S$  affects not only  $v_i$  and  $v_j$ , but also the neighbors of these two nodes [9]. Therefore, the graph adversarial attack model can be written as the following optimization problem:

$$\begin{aligned} & \text{maximize} && \left\| (S')^k - S^k \right\|_F^2 \triangleq \ell_1(A', \alpha) \\ & \text{subject to} && A'_{ii} = 1, \quad i = 1, \dots, N \\ & && A'_{ij} \in \{0, 1\} \text{ for } i \neq j \\ & && \|A' - A\|_0 \leq 2\delta, \end{aligned} \quad (2)$$

where the optimization variable is the  $N \times N$  symmetric matrix  $A'$ . According to the definition of  $S$  in Eq. 1, we denote the objective as a function of  $A'$  and  $\alpha$ , *i.e.*,  $\ell_1(A', \alpha)$ . The constant  $k$  is a given small integer, indicating neighbors within  $k$  hops (instead of that with the exact  $k$ -hop) are considered in  $S^k$  since  $A$  is with self-loops. When targeting on localized kernels like GCN, we prefer to choose

$k = 1$  or  $2$ ; while aiming to capture higher-order structural patterns, larger  $k$  is recommended. We also have  $2\delta$  with  $0 < \delta \ll |E|$  for the budget constraint on undirected graphs, which is a typical perturbation budget form used in most previous works [19].

### 3 METHODOLOGY

Although the objective function  $\ell_1(A', \alpha)$  described in Problem (2) directly shows the difference between the original graph filter and the perturbed one, it has two significant disadvantages. First, it is affected by the parameter  $\alpha$  of graph filter. Clearly, different choices of  $\alpha$  result in different attack strategies for Problem (2). This would largely hurt our model's generality as we are in favor of one stable model for different choices of graph filters in various graph models. Second, computing  $\ell_1(A', \alpha)$  is time-consuming, thus dramatically slowing down the general solvers for Problem (2), as well as limiting its scalability. The most expensive step in computing  $\ell_1$  is the eigenvalue decomposition of  $S'$ , which requires  $O(N^3)$  flops.

We therefore aim to find an alternative for  $\ell_1(A', \alpha)$ , which can be computed efficiently while also being immune to the change of  $\alpha$ . We first relax  $\ell_1(A', \alpha)$  to its lower bound  $\ell_2(\lambda')$  which is independent of  $\alpha$  (§ 3.1). Next, we give a approximate solution to compute this lower bound  $\ell_2(\lambda')$  (§ 3.2). A detailed description of how to select adversarial edges is provided for solving the relaxed problem (§ 3.3). Finally, we show that the proposed model is flexible to be extended when more knowledge can be accessed (§ 3.4).

#### 3.1 A practically viable lower bound

The first observation on the eigenvalues of the graph filter  $S$  is the following lemma.

**LEMMA 1.**  $\lambda$  is an eigenvalue of  $S = D^{-\alpha}AD^{-1+\alpha}$  if and only if  $\lambda$  and  $u$  solve the generalized eigenproblem  $Au = \lambda Du$ .

This lemma can be simply proved because  $D^{-\alpha}AD^{-1+\alpha}(D^{1-\alpha}u) = \lambda(D^{1-\alpha}u)$ . It reveals that the eigenvalues of  $S$  are independent of the choice of  $\alpha$ . Hence, a lower bound on  $\ell_1(A', \alpha)$  that involves only the eigenvalues will help to solve the maximization Problem (2).

**THEOREM 1.** The function  $\ell_1(A')$  is lower bounded by

$$\ell_1(A', \alpha) \geq \left( \sqrt{\sum_{i=1}^N (\lambda'_i)^{2k}} - \sqrt{\sum_{i=1}^N \lambda_i^{2k}} \right)^2 \triangleq \ell_2(\lambda'), \quad (3)$$

where  $\lambda_i$  and  $\lambda'_i$  are the  $i$ -th generalized eigenvalue of  $A$  and  $A'$ , respectively, i.e.,  $Au_i = \lambda_i Du_i$  and  $A'u'_i = \lambda'_i D'u'_i$ . We assume that both eigenvalue sequences are numbered in a nonincreasing order.

The  $i$ -th generalized eigenvalue of  $A'$  (i.e., the  $i$ -th eigenvalue of  $S'$ ) is upper bounded by

$$\lambda'_i = \lambda_i(S') \leq \frac{1}{d'_{\min}} \cdot \lambda_i(A'), \quad (4)$$

where  $d'_{\min}$  is the smallest degree in  $G'$ ,  $\lambda_i(S')$  and  $\lambda_i(A')$  are the  $i$ -th eigenvalue of  $S'$  and  $A'$ , respectively. This suggests that the eigenvalues of  $S'$  are always bounded by the eigenvalues of  $A'$ .

**PROOF.** According to the triangle inequality,  $\ell_1(A')$  is lower bounded by

$$\begin{aligned} \|(S')^k - S^k\|_F^2 &\geq (\|(S')^k\|_F - \|S^k\|_F)^2 \\ &= \left( \sqrt{\sum_{i=1}^n \lambda_i(S')^{2k}} - \sqrt{\sum_{i=1}^n \lambda_i(S)^{2k}} \right)^2 \\ &= \left( \sqrt{\sum_{i=1}^N (\lambda'_i)^{2k}} - \sqrt{\sum_{i=1}^N \lambda_i^{2k}} \right)^2, \end{aligned}$$

where the last step follows from Lemma 1.

By applying the Weyl's inequalities (Cf. Theorem 4 in the appendix [18]) twice, and according to  $(d'_1)^{-\alpha} \geq (d'_2)^{-\alpha} \geq \dots \geq (d'_N)^{-\alpha}$  and  $(d'_1)^{-1+\alpha} \geq (d'_2)^{-1+\alpha} \geq \dots \geq (d'_N)^{-1+\alpha}$  because  $\alpha \in [0, 1]$ , we have

$$\begin{aligned} \lambda_i(S') &= \lambda_i(D'^{-\alpha}A'D'^{-1+\alpha}) \\ &\leq \lambda_1(D'^{-\alpha}) \lambda_i(A'D'^{-1+\alpha}) \\ &\leq \lambda_1(D'^{-\alpha}) \lambda_i(A') \lambda_1(D'^{-1+\alpha}) \\ &= d_1'^{-\alpha} \lambda_i(A') d_1'^{-1+\alpha} \\ &= \frac{1}{d'_{\min}} \lambda_i(A'), \end{aligned}$$

where  $\lambda_1$  is the largest eigenvalue and  $d'_1 = d'_{\min}$  is the smallest degree in  $G'$ .  $\square$

In terms of the spectral graph theory [9], the Frobenius norm  $\|S^k\|_F$  is the root-mean-square of the graph spectrum; thus, the lower bound  $\ell_2(\lambda')$  can be used to describe the spectral change. It should also be noted that the spectrum of  $S$  of different graphs (with no isolated vertices) are bounded in the same range  $[-1, 1]$  [9], making them more comparable when measuring their difference (this is also the reason for choosing the  $\ell_1$  objective). In addition, Eq. (3) is valid for any symmetric matrices  $S$  and  $S'$ ; hence, the lower bound  $\ell_2(\lambda')$  holds for different types of networks (e.g. weighted or unweighted, signed or unsigned) and different perturbation scenarios (e.g. adding or deleting edges, adjusting edge weights). Accordingly the problem of maximizing  $\ell_1(A', \alpha)$ , i.e., Problem (2), can be properly relaxed to a problem of maximizing its lower bound  $\ell_2(\lambda')$ .

#### 3.2 Approximating perturbed eigensolution

However, although  $\ell_2(\lambda')$  is a desirable lower bound for the above reasons, it is still no easier to evaluate than  $\ell_1(A', \alpha)$ . The generalized spectrum of  $A$  requires only one-time computation and thus can be assumed to be known. The main computational bottleneck, on the other hand, is the computation of the generalized eigenvalues of  $A'$ , as these need to be re-evaluated for every possible set of flipped edges. To alleviate this burden, we first observe that the modification to the graph is relatively small – i.e.,  $\delta \ll |E|$  – and thus that the first-order perturbation analysis [30] is accurate enough for our purposes. Accordingly we provide an efficient first-order approximation of the change in the eigenvalues of  $S'$ .

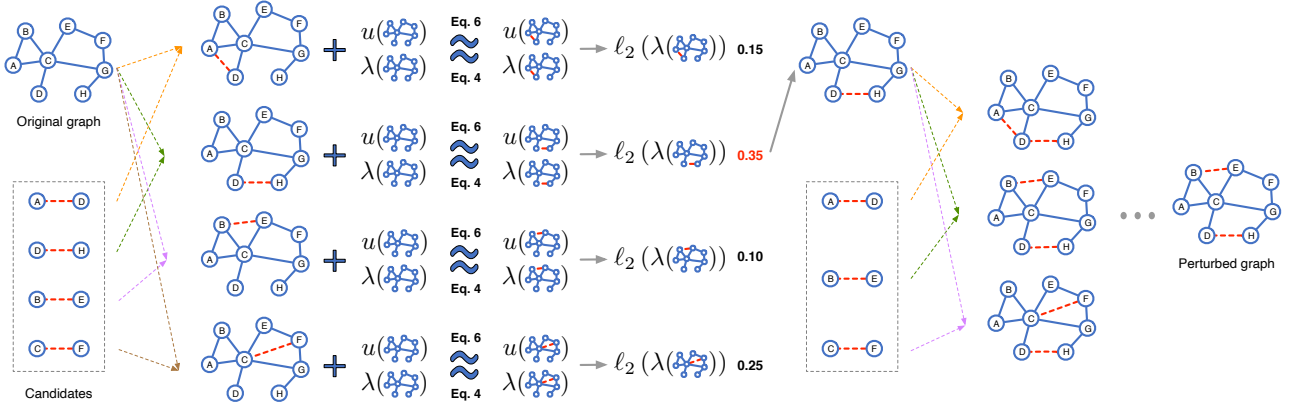


Figure 2: An illustrative example of the proposed attack procedure on graphs, in which the budget constraint  $\delta$  is set to be 2.

**THEOREM 2.** Let  $\Delta A = A' - A$  and  $\Delta D = D' - D$  be the perturbations of  $A$  and  $D$ , respectively. Moreover, the number of non-zero entries of  $\Delta A$  and  $\Delta D$  are assumed to be much smaller than that of  $A$  and  $D$ . Let  $(\lambda_k, u_k)$  be the  $k$ -th pair of generalized eigenvalues and eigenvectors of  $A$ , i.e.,  $Au_k = \lambda_k Du_k$ . We assume that these eigenvectors are properly normalized such that they satisfy  $u_j^T Du_i = 1$  if  $i = j$  and 0 otherwise. Thus, the  $k$ -th generalized eigenvalue  $\lambda'_k = \lambda_k + \Delta\lambda_k$  can be approximated by

$$\lambda'_k \approx \lambda_k + u_k^T (\Delta A - \lambda_k \Delta D) u_k.$$

Moreover, when the eigenvalues are distinct, the  $k$ -th generalized eigenvector  $u'_k$  of  $A'$  can be approximated by

$$u'_k \approx \left(1 - \frac{1}{2} u_k^T \Delta D u_k\right) u_k + \sum_{i \neq k} \frac{u_i^T (\Delta A - \lambda_k \Delta D) u_k}{\lambda_k - \lambda_i} u_i.$$

More specifically, when only one edge  $\{p, q\}$  is flipped,  $\Delta A$  has only two non-zero elements, i.e.,  $\Delta A_{pq} = \Delta A_{qp} = 1 - 2A_{pq}$ . In this case, the above approximations can be further simplified as

$$\lambda'_k \approx \lambda_k + \Delta A_{pq} (2u_{kp} \cdot u_{kq} - \lambda_k (u_{kp}^2 + u_{kq}^2)) \quad (5)$$

$$u'_k \approx \left(1 - \frac{1}{2} \Delta A_{pq} (u_{kp}^2 + u_{kq}^2)\right) u_k + \sum_{i \neq k} \frac{\Delta A_{pq} (u_{ip} u_{kq} + u_{iq} u_{kp} - \lambda_k (u_{ip} u_{kp} + u_{iq} u_{kq}))}{\lambda_k - \lambda_i} u_i \quad (6)$$

where  $u_{kp}$  is the  $p$ -th entry of the vector  $u_k$ .

When only one edge is flipped, the approximation of one specific eigenvalue  $\lambda'_k$  requires only  $O(1)$  flops to compute, as shown in Eq. (5). However, computational cost associated with re-evaluating of the eigenvectors is still higher than we would like: specifically, the computation of Eq. (6) requires  $O(N^2)$  flops for only one eigenvector  $u'_k$ . Worse yet Eq. (6) is valid only when all eigenvalues are distinct, which is not guaranteed in practice. Therefore, we propose to approximate the perturbed eigenvectors using only one power iteration as the following theorem does.

**THEOREM 3.** Let  $\Delta A = A' - A$  and  $\Delta D = D' - D$  denote the perturbations of  $A$  and  $D$ , respectively. Moreover, the number of non-zero entries of  $\Delta A$  and  $\Delta D$  are assumed to be much smaller than

that of  $A$  and  $D$ . Let  $u_k$  be the  $k$ -th generalized eigenvector of  $A$  with generalized eigenvalue  $\lambda_k$ . We first assume that the eigenvectors are properly normalized, such that  $\|u_k\|_2 = 1$ . The  $k$ -th generalized eigenvector  $u'_k$  can then be approximated by

$$u'_k \approx \begin{cases} \text{sign}(\lambda_k) u_k + \frac{\Delta C u_k}{|\lambda_k|} & \text{if } \lambda_k \neq 0 \\ \frac{\Delta C u_k}{\|\Delta C u_k\|_2} & \text{if } \lambda_k = 0. \end{cases} \quad (7)$$

where  $\Delta C = (D + \Delta D)^{-1} (A + \Delta A) - D^{-1} A$ . Specifically, when one edge  $\{p, q\}$  is flipped, only the  $p$ -th and  $q$ -th elements of  $u'_k$  will be changed because only specific elements of  $\Delta C$  are non-zero, i.e.,

$$\Delta C_{ij} = \begin{cases} A'_{pj}/D'_{pp} - A_{pj}/D_{pp}, & \text{if } j \in \mathcal{N}(p) \cup \{p, q\} \\ A'_{qj}/D'_{qq} - A_{qj}/D_{qq}, & \text{if } j \in \mathcal{N}(q) \cup \{p, q\} \\ 0, & \text{otherwise.} \end{cases}$$

**PROOF.** According to one iteration of power iteration, when  $\lambda_k \neq 0$ ,

$$\begin{aligned} u'_k &\approx \frac{(D + \Delta D)^{-1} (A + \Delta A) u_k}{\|(D + \Delta D)^{-1} (A + \Delta A) u_k\|_2} \\ &= \frac{(D^{-1} A + \Delta C) u_k}{\|(D^{-1} A + \Delta C) u_k\|_2} \\ &= \frac{\lambda_k u_k + \Delta C u_k}{\|\lambda_k u_k + \Delta C u_k\|_2} \\ &= \frac{\lambda_k u_k + \Delta C u_k}{\sqrt{\lambda_k^2 u_k^T u_k + 2\lambda_k u_k^T \Delta C u_k + u_k^T \Delta C^T \Delta C u_k}} \\ &\approx \frac{\lambda_k u_k + \Delta C u_k}{|\lambda_k|} = \text{sign}(\lambda_k) u_k + \frac{\Delta C u_k}{|\lambda_k|}. \end{aligned} \quad (8)$$

When  $\lambda_k = 0$ , we can derive from (8) that  $u'_k \approx (\Delta C u_k) / (\|\Delta C u_k\|_2)$ .  $\square$

When only one edge is flipped, Eq. (7) suggests that the approximation of the perturbed eigenvector requires only  $O(N)$  flops, which is far more efficient than  $O(N^2)$  using Eq. (6). In addition, the evaluation of  $u'_k$  in Eq. (7) involves only the corresponding eigenvalues  $\lambda_k$ , which removes the strict assumption regarding distinct eigenvalues.

### 3.3 Selection of adversarial edges

Up to this point, we have aimed to flip  $\delta$  edges so that  $\ell_2(\lambda')$  is maximized. Since the number of candidates would be too large if  $\delta$  links were chosen, we adopt a greedy strategy as suggested in previous works [43, 44] to flip one edge during each step. We first form a candidate set by randomly sampling several edge pairs, as in [3]. Our greedy strategy based on a randomly selected candidate set involves three steps: (i) for each candidate, compute its impact  $\ell_2(\lambda')$  on the original graph, such that the eigenvalues can be approximated via Eq. (5); (ii) flip the candidate edge that scores highest on this metric; and (iii) recompute the eigenvalues and eigenvectors after each time an edge is flipped (here we use approximation via Eq. (5) and Eq. (7) rather than accurate recomputation). These steps are repeated until the budget  $\delta$  has been flipped. Figure 2 briefly illustrates such adversarial attack procedure.

**Eigensolution approximation with restart.** In the strategy outlined above, the approximation of the statistic in step (iii) is efficient, as demonstrated in § 3.1. However, it inevitably leads to serious error accumulation as more edges are flipped, since the eigenvalues and eigenvectors are approximated on incremental updates. A straightforward solution is to reset the aggregated error (*i.e.*, recompute the exact eigensolutions) over time; thus, the question of when to restart should be answered carefully. Note that in Theorem 2, the perturbed eigenvectors must be properly normalized as  $u_i'^T D' u_i' = 1$  if  $i = j$ . Here, we can perform an orthogonality check to verify whether the eigenvectors have been adequately approximated. Theoretically, if the perturbed eigenvectors are approximately accurate and normalized to  $u'^T D' u'$ , then  $U'^T D' U'$  will be close to the identity matrix. Thus, we propose to use the average of the magnitudes of the non-zero off-diagonal terms of  $U'^T D' U'$  to infer the approximation error of the perturbed eigenvectors, *i.e.*

$$\epsilon = \frac{1}{N(N-1)} \sum_{i=1}^N \sum_{j \neq i} |I'_{ij}|, \quad (9)$$

where  $I' = U'^T D' U'$ . The smaller the value of  $\epsilon$ , the more accurate our approximation. Therefore, the approximation error  $\epsilon$  is monitored in every iteration, and restart (*i.e.* recomputing the exact eigensolutions of the perturbed matrix) is performed when the error exceeds a threshold  $\theta$ . Intuitively, this allows us to reduce time complexity as well as ensure approximation accuracy.

The overall attack strategy is presented in Algorithm 1. Compared with the exact solution that costs  $\mathcal{O}(N^3)$ , we here present two approximate solutions. On one hand, the approximate solution without restart mechanism will reduce the runtime complexity to  $\mathcal{O}(N^2)$  but it still can give us comparable results (see the performance of *Ours-r* in the experiments). On the other hand, by adding the restart mechanism (*i.e.*,  $0 < r < \delta$ , where  $r$  is the number of restart), our solution will be slower but still speed up with a ratio  $\sim \delta/r$  compared with the exact one and achieve better performance (see the performance of *Ours* in the experiments).

One limitation of our solution is that the candidate set of adversarial edges is formed by randomly sampling edge pairs. This randomness introduces another approximation but works well in practice (see the results with standard deviation in Table 1 and

---

**Algorithm 1** Overall attack strategy via eigensolution approximation with restart.

---

**Input:** Graph  $G = (A)$ , perturbation budget  $\delta$ , restart threshold  $\theta$ .  
**Output:** Modified Graph  $G' \leftarrow (A')$ .

```

1:  $A' \leftarrow A, D' \leftarrow D$ ;
2: Solve the exact eigensolutions:  $A' u' = \lambda' D' u'$ ;
3:  $\text{Cand} \leftarrow \text{candidate}(A')$ ;
4: while  $\|A' - A\|_0 \leq 2\delta$  do
5:    $e' \leftarrow \underset{e \in \text{Cand}}{\text{argmax}} \ell_2(e)$ , which is approximated via Eq. 5;
6:    $A', D' \leftarrow \text{insert or remove } e' \text{ to/from } A'$ ;
7:   Approximately update eigenvalue  $\lambda'$  via Eq. 5 and update
   eigenvector  $u'$  via Eq. 7;
8:   if  $u' \neq \mathbf{0}$  then
9:     Normalize the perturbed eigenvector  $u'$  s.t.  $u_j'^T D u_i' = 1$  if
      $i = j$ ;
10:    Compute  $\epsilon$  via Eq. 9;
11:    if  $\epsilon > \theta$  then
12:      Recompute the exact eigensolutions;
13:    end if
14:  else
15:    Recompute the exact eigensolutions;
16:  end if
17:   $\text{Cand} \leftarrow \text{remove } e'$ ;
18: end while
19:  $G' \leftarrow (A')$ .
```

---

Figure 6 in the appendix). We leave it as future works to investigate the candidate selection problems further.

### 3.4 Extension to different knowledge levels

Our proposed adversarial manipulation can also be easily extended to boost performance when additional knowledge (*e.g.*, model structure, learned parameters, queries) is available. One straightforward way of doing this would be adopt  $\ell_2(\lambda')$  as a regularization term. Thereby, complementary to other types of adversarial attacks (*e.g.*, white-box or query-based black-box), the proposed attack model facilitates rich discrimination on global changes in the spectrum.

As an example, assume that our goal is to attack a graph convolutional network (GCN) designed for the semi-supervised node classification task. The attacker only has query access to the GCN model, but knows nothing about either the detailed structure or the learned parameters. The attacker is able to alter both the graph structure and the node attributes, and its goal is to misclassify a specific node  $v_i$ . In this case, a surrogate model is built with all non-linear activation function removed [43]; this is denoted as  $Z = \text{softmax}(S^k X W)$ , where  $X$  denotes the feature matrix and  $W$  represents the learned parameters. Therefore, the combined attack model tries to solve the following optimization problem:

$$\text{maximize}_{c \neq c_0} \max((S'^k X' W)_{v_i c} - (S'^k X W)_{v_i c_0}) + \gamma \ell_2(\lambda')$$

where the variables are the graph structure  $A'$  and the feature matrix  $X'$ , the scalar  $c_0$  denotes the true label or the predicted label for  $v_i$  based on the unperturbed graph  $G$ , while  $c$  is the class of  $v_i$  to which the surrogate model assigns. The constant  $\gamma > 0$  is a

regularization parameter. Note that this case can also be considered as an extension to targeted attack. Besides, our method is also flexible to be extended when more information can be accessible. For example, when node features are available, we can alternatively add a term w.r.t the feature distance between two end nodes of a selected edge to our objective.

## 4 EXPERIMENTS

In this section, we evaluate the benefits of our proposed method with the aim of answering the following questions: 1). How far is the gap between the initial formulation of Problem (2) and our approximate solution; 2). Can our method attack node classification task; 3). Will our method perform well when attacking graph classification task; 4). Will our method still work on defensive models; 5). Can our method be extended to white-box or targeted attack? 6). Is our method sensitive to the choices of hyperparameters?

**Datasets.** In the following experiments, we use three real-world datasets for node-level attack evaluation: Cora-ML [22], Citeseer [28] and Polblogs [1] when performing node-level attack. All of these have been preprocessed in the previous work [11]. When performing graph-level attack, we evaluate on two benchmark protein datasets for graph classification: Enzymes [5] and Proteins [12].

**Baselines.** Since few studies have investigated the query-free black-box attack setting, we compare our approach against the following baselines. *Rand.*: randomly flips edges; *Deg./Betw./Eigen.* [3]: the flipped edges are selected on the decreasing order of the sum of the degree/betweenness/eigenvector centrality; *DW*: a black-box attack method designed for DeepWalk [3]; and *GPGD* (Graph Projected Gradient Descent), an optimization-based method whose objective is adopted as  $\ell_1$  ( $A'$ ) under our setting [37]. A recent work of black-box attack [6] is also considered but it fails to get results within one entire day.

In our implementation, we only involve two hyper-parameters: the spatial coefficient  $k$  is set to be 1 and the restart threshold  $\theta$  is set to be 0.03. In what follows, the reported results are all averaged over 10 trials with a random training/validation/testing split and random weight matrix initialization. More detailed information about the datasets and implementations can be found in the appendix.

### 4.1 Approximation quality

To estimate the approximation error of the original objective  $\ell_1$  and the approximated one, we mainly suffer from two error accumulation: the first occurs when converting the actual objective  $\ell_1$  to its surrogated lower bound  $\ell_2$ , while the second is caused by the eigensolution approximation (note that we ignore the sampling error when forming a candidate set because [3] has validated that it works well in practice). We first evaluate the accuracy of eigensolution approximation by flipping 10 edges (100 trials are conducted) in synthetic graphs and then compare the true eigenvalues with our approximated ones. The example synthetic random graphs (*i.e.*, Erdős-Rényi [4], Barabási-Albert [2], Watts-Strogatz [34] and Powerlaw configuration [17]) are generated with 1K nodes and their parameters are chosen so that the average degree is approximately 10 (details of these synthetic datasets can be found in the appendix). Figure 3 presents our approximation accuracy compared with the true eigenvalues, where the trend of red plus symbols shows that

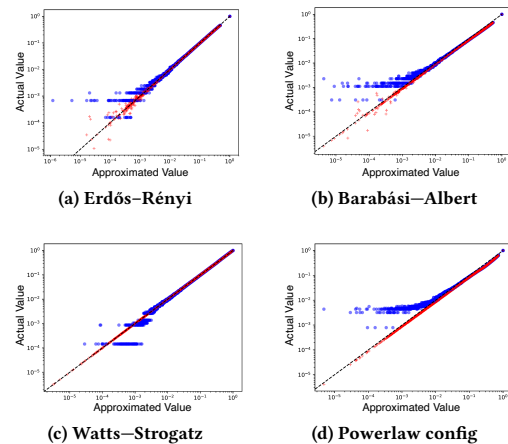


**Figure 3: The true eigenvalues (y-axis) are plotted against the approximations (x-axis) in log scale. The red plus symbols represent our approximations with restart, while the blue circles denote the approximations without restart.**

our approximated eigenvalues via eigensolution approximation with restart (Cf. § 3.3) accurately match the actual values. As an ablation, approximations by removing the restart mechanism are plotted by blue circle symbols in Figure 3, which can be observed a tendency of overestimating the change in eigenvalues before and after attacks.

Based on our accurate eigenvalue approximation with restart, we further want to see how far is the gap between  $\ell_2$  and  $\ell_1$ . We compute their Pearson and Spearman correlation coefficients on three real-world datasets. Accordingly, we have  $Pearson(\ell_1, \ell_2) = 0.89$  and  $Spearman(\ell_1, \ell_2) = 0.91$  on Cora-ML;  $Pearson(\ell_1, \ell_2) = 0.91$  and  $Spearman(\ell_1, \ell_2) = 0.93$  on Citeseer and  $Pearson(\ell_1, \ell_2) = 0.85$  and  $Spearman(\ell_1, \ell_2) = 0.93$  on Polblogs. These statistics suggest the linear and monotonic relationships between the actual objective and our approximation.

### 4.2 Attack effectiveness

**Node-level attack.** When attacking GCN [20], Node2vec [15] and Label Propagation [42] on node classification task, our setting is the so-called poisoning attack, where the target models are re-trained following perturbations. We set the size of the sampled candidate set as 20K and allow 10% of  $|E|$  edges to be modified. We split every dataset as training/validation/testing = 0.1:0.1:0.8. As Table 1 shows, on all three victim models, our method achieves the best performance across all datasets. The ablation study on *Ours-r* further highlights the significance of the restart strategy, which helps to reduce our approximation error by a substantial amount. Moreover, we find that it is difficult for intuitive heuristics like *Deg.*, *Betw.* and *Eigen.* to discover adversarial edges (see more analyses in the appendix). Besides, *DW* suffers from a transferability problem because it is specially designed for DeepWalk [27]. *GPGD* also does not perform very well; this bias may be caused by the relaxation from a discrete optimization problem to a continuous one. Table 2 further shows that under increasing perturbation rates of 5%, 10%,

and 15%, our attack is able to do more damage to GCN on the node classification task while still achieves the best performance. Furthermore, when the perturbation rate is not very high, our solution without restart is already good enough to mount attacks. Additionally, the white-box attack models of GCN are trained for reference, where we perform *GPGD* attack based on the cross entropy loss of GCN as [37] suggested. Since few works have studied the white-box attacks on node embedding models and diffusion models, we here only report the transferability of white-box attacks w.r.t GCN to Node2vec and Label Propagation in parentheses in Table 1. From which we can see such kind of white-box attack model performs very well on Cora-ML and Citeseer when attacking GCN while it fails when attacking other victim models.

**Analysis of objective function.** In addition, we compare with some candidates of objective under the same setting of query-free black-box attacks to validate the decent choice of  $\ell_2(\lambda')$ , which is proposed to capture the adversarial structural changes by the graph filter  $S$ . Other candidates, like  $\|A' - A\|_F^2$ , obviously cannot distinguish the cases when the same number of edges are flipped, while  $\ell_1^* = \|(A')^k - A^k\|_F^2$  only considers the number of walks between two nodes of length  $k$ . Moreover,  $\ell_2^* = \left\| \sum_{i=1}^k ((A')^i - A^i) \right\|_F^2$  is computationally expensive, also  $\ell_2^*$  and the above candidates' spectrum are not bounded in the same range across different graphs. We

**Table 2: Decrease in Macro-F1 score with different perturbation rates when attacking GCN on Cora-ML.**

	5%	10%	15%
<i>Rand.</i>	0.75	1.97	2.41
<i>Deg.</i>	0.59	1.12	1.34
<i>Betw.</i>	0.63	1.22	1.45
<i>Eigen.</i>	0.30	0.28	1.12
<i>DW</i>	0.34	0.85	1.23
<i>GPGD</i>	3.94	4.22	5.03
<i>Ours-r</i>	<b>4.43</b>	5.02	5.77
<i>Ours</i>	4.30	<b>5.27</b>	<b>6.40</b>

additional present the results (see Table 3) of utilizing these candidates to attack node classification task as the setting of node-level attack. From the results in Table 3, we can see that the superiority of our model, which constantly demonstrates the effectiveness of our objective function.

**Table 3: The experimental results of other objective functions of node-level attacks against three types of victim models. We report the decrease in Macro-F1 score (in percent) on the test set after the attack.**

		$\ell_1^*$	$\ell_2^*$	<i>Ours</i>
Cora-ML	GCN	1.92	1.72	<b>5.27</b>
	Node2vec	8.05	8.14	<b>8.29</b>
	Label Prop.	5.32	5.37	<b>7.13</b>
Citeseer	GCN	1.65	2.27	<b>3.98</b>
	Node2vec	8.64	9.05	<b>9.32</b>
	Label Prop.	7.09	5.41	<b>8.16</b>
Polblogs	GCN	2.65	2.92	<b>5.32</b>
	Node2vec	3.68	3.43	<b>3.79</b>
	Label Prop.	4.80	4.20	<b>6.14</b>

**Table 4: Graph-level attacks against GIN and Diffpool. We report the decrease in the Macro-F1 score (in percent) on test set. Higher numbers indicate better performance.**

	Proteins		Enzymes	
	GIN	Diffpool	GIN	Diffpool
<i>Rand.</i>	9.05	24.13	32.76	38.09
<i>Deg.</i>	9.31	11.27	34.38	17.48
<i>Betw.</i>	12.50	9.87	34.75	9.51
<i>Eigen.</i>	8.00	11.03	<b>40.25</b>	17.74
<i>DW</i>	13.44	12.71	38.76	13.55
<i>GPGD</i>	9.49	14.53	35.63	20.32
<i>Ours-r</i>	12.81	24.87	37.46	<b>40.18</b>
<i>Ours</i>	<b>13.53</b>	<b>24.88</b>	39.90	39.62

**Table 1: The experimental results with standard deviation of node-level attacks against three types of victim models. We report the decrease in Macro-F1 score (in percent) on the test set after the attack is performed; the higher the better. We also report the Macro-F1 on the unattacked graph.**

Victim	Attacker (Unattacked)	<i>Rand.</i>	<i>Deg.</i>	<i>Betw.</i>	<i>Eigen.</i>	<i>DW</i>	<i>GPGD</i>	<i>Ours-r</i>	<i>Ours</i>	White-box	
		Cora-ML	GCN	0.82±0.8	1.97±0.8	1.12±0.4	1.22±0.4	0.28±0.3	0.85±0.3		4.22±0.6
	Node2vec	0.79±0.8	6.37±1.8	5.40±1.6	3.33±1.0	2.84±1.0	3.25±1.3	5.33±1.8	6.92±1.0	<b>8.29±1.0</b>	(1.43±0.9)
	Label Prop.	0.80±0.7	4.10±1.3	2.45±0.7	2.71±0.8	2.07±0.7	1.79±0.9	4.28±1.6	6.02±0.9	<b>7.13±0.9</b>	(1.05±1.0)
Citeseer	GCN	0.66±1.4	2.02±0.6	0.16±0.4	0.70±0.4	0.64±0.4	0.21±0.4	2.14±0.9	3.16±0.6	<b>3.98±0.5</b>	6.42±0.6
	Node2vec	0.60±1.5	7.47±2.3	7.47±1.6	3.47±2.6	4.87±1.5	2.54±2.5	5.26±1.9	8.32±2.5	<b>9.32±2.6</b>	(0.12±1.0)
	Label Prop.	0.64±0.8	7.12±1.3	3.47±0.8	6.00±1.7	5.36±0.6	3.00±0.8	5.14±1.9	7.79±0.9	<b>8.16±0.9</b>	(2.47±1.2)
Polblogs	GCN	0.96±0.7	1.91±1.5	0.03±0.2	1.72±0.6	0.67±0.5	0.01±0.4	2.35±1.8	4.30±1.2	<b>5.32±1.1</b>	3.88±1.1
	Node2vec	0.95±0.3	3.01±0.7	0.04±0.6	3.07±0.6	1.84±0.3	0.18±0.4	2.49±0.6	2.74±0.5	<b>3.79±0.5</b>	(2.13±0.4)
	Label Prop.	0.96±0.5	4.99±0.7	0.08±0.4	3.45±0.7	2.15±0.3	0.37±0.5	4.15±0.8	5.84±0.7	<b>6.14±0.7</b>	(2.28±0.5)

**Table 5: Decrease in Macro-F1 score of black-box attacks against EdgeDrop [11], Jaccard [36] and SVD [41] on Cora-ML.**

	w/o defense	EdgeDrop	Jaccard	SVD
<i>GPGD</i>	4.22	6.04	3.94	3.47
<i>Ours</i>	5.27	7.11	4.71	4.02

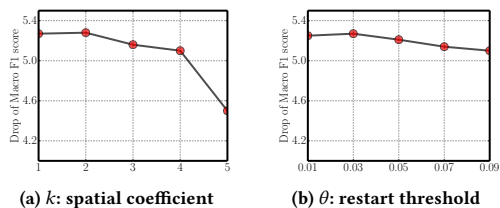
**Table 6: Extension to *Nettack*. We report the average decrease in prediction confidence (in percent) of true labels and the misclassification rate in parentheses.**

	Cora-ML	Citeseer	Polblogs
<i>Nettack</i>	55.70 (0.53)	63.41 (0.60)	5.16 (0.23)
<i>Our extension</i>	<b>59.75 (0.57)</b>	<b>65.58 (0.63)</b>	<b>5.40 (0.23)</b>

**Graph-level attack.** To probe our attack method’s ability on the graph classification task, we conduct evaluations on Enzymes and Proteins. We use GIN [38] and Diffpool [40] as our target models due to their superiority on graph classification and follow their settings, including the training/validation/testing split. The attacker is allowed to modify 20% of the  $|E|$  edges. Table 4 demonstrates the significance of our method (+2.65% in terms of Macro-F1). It is also interesting to note that *Ours-r* (without restart) sometimes performs very well, indicating that we can apply a version with lower complexity  $\mathcal{O}(N^2)$  in practice yet not sacrificing accuracy.

**Attacks on Defensive models.** We further validate the effectiveness of our proposed model by conducting attacks against three defensive models: EdgeDrop [11], Jaccard [36] and SVD [41]. We utilize GCN as the backbone classifier and test on node classification task. We compare our method with the strongest competitor *GPGD*. The experimental settings are the same as those used in node-level attack. The results in Table 5 demonstrate that our method outperforms *GPGD* in terms of its ability to attack the defensive models. We can see that EdgeDrop cannot effectively defend against our attack, while the two pre-processing defense approaches (Jaccard and SVD) can defend against our attack to a certain extent.

**Extension when additional knowledge is available.** We here determine whether our attack can be successfully extended as the example in § 3.4. Specifically, we aim at extending to *Nettack* [43] and follow their targeted attack settings. We evaluate on node-level attack and split every dataset as training/validation/testing =

**Figure 4: Parameter analysis for node classification task.**

0.1:0.1:0.8. We randomly select 30 nodes from the test set that have been correctly classified and mount targeted attacks on these nodes. We set the perturbation budget for each node to 2. From Table 6, we see our extension can further drop 4.84% in terms of prediction confidence and increase 4.18% in terms of misclassification rate on average, demonstrating the its flexibility.

**Parameter Analysis.** Our algorithm involves two hyperparameters: namely, the spatial coefficient  $k$  and restart threshold  $\theta$ . We use grid search to find their suitable values on Cora-ML and present here for reference (see Figure 7). Better performance can be obtained when  $k \in \{1, 2\}$  and  $\theta \leq 0.03$ . The observation that our model’s superiority when  $k \leq 2$  is consistent with many conclusions of graph over-smoothing problem [21, 23]. Remarkably, our model can still achieve relatively good performance (*i.e.*, better than the baseline methods) regardless of how hyperparameters are changed.

## 5 RELATED WORKS

Adversarial attacks on graphs can be classified as white-box, gray-box and black-box attacks [19]. Getting access to full knowledge (*e.g.*, model architecture and learned parameters) about a victim model, the adversaries generally prefer white-box attacks [7, 31, 33, 36, 37]. The training of most white-box attacks involves a gradient w.r.t the input of the model [7, 33, 36, 37]. In practical scenarios, however, adversaries may not be able to acquire such perfect knowledge, preventing them from adopting gradient-based algorithms directly. Gray-box attacks are proposed under such consideration where the attackers are usually familiar with the architecture of the victim models [8, 19]. One common method is to train substitute models as surrogates to estimate the information of the victim models. Zügner et al. [43, 44] assume that the victim model is graph neural network-based, and build a simple surrogate model by removing all non-linearities in graph neural network as an approximation. However, such GNN-based surrogate models rely on labels for training, which is often unrealistic as many graphs in the wild are unlabeled. Bojchevski and Günnemann [3] approach an effective surrogate loss of DeepWalk via the approximation theory of eigenvalue perturbation. Despite its tractability, the performance of such attack suffers the approximation error of surrogate models.

Whereas, so long as less or no information is exposed, the adversaries will have to adopt black-box attacks instead. Under these circumstances, the adversaries can only access the model as an oracle and may query some or all of the examples to obtain continuous-valued predictions or discrete classification decisions. Working under such limitations, Dai et al. [11] employ a reinforcement learning-based method and a genetic algorithm, where the results from queries serve as their learning direction. However, their modifications are restricted to edge deletion, and the transferability was also not well studied. Despite its many practical merits, the query-based black-box attack requires numerous queries, which makes the whole procedure costly in terms of both money and time and can arouse suspicion within the target system.

Unlike the above-mentioned counterparts, the query-free black-box attack is a much more challenging scenario in which the adversaries have no ability to send queries to the underlying learning model. The most similar work to ours is Chang et al. [6], which is also a query-free attack method based on graph signal processing.

However, the objective function they used is dependent on the type of the embedding model (*i.e.*, GCN-based or sampling-based). In our work, the proposed query-free black-box scheme can be applicable to various graph-learning models, which is a more strict setting.

## 6 CONCLUSION

We introduced a query-free black-box adversary for graph learning models, which can be formulated as a constrained optimization problem associated with the graph filter. We target at a relaxation relying only on the graph spectrum and approximate via eigenvalue perturbation theory. We suggest adopting a greedy algorithm to solve the relaxation problem. Numerical experiments on various tasks and datasets demonstrate that the proposed attack model is both effective and scalable. For future work, we aim to extend our method to more white-box and query-based black-box attacks.

## REFERENCES

- [1] Lada A. Adamic and Natalie Glance. 2005. The Political Blogosphere and the 2004 U.S. Election: Divided They Blog. In *Proceedings of the 3rd international workshop on Link discovery, LinkKDD 2005, Chicago, Illinois, USA, August 21-25, 2005*.
- [2] Réka Albert and Albert-László Barabási. 2002. Statistical Mechanics of Complex Networks. *Reviews of Modern Physics* 74 (2002), 47–97. <https://doi.org/10.1103/RevModPhys.74.47>
- [3] Aleksandar Bojchevski and Stephan Günnemann. 2019. Adversarial Attacks on Node Embeddings via Graph Poisoning. In *Proceedings of the 36th International Conference on Machine Learning, ICML 2019, 9-15 June 2019, Long Beach, California, USA*.
- [4] Béla Bollobás. 2013. *Modern graph theory*. Vol. 184. Springer Science and Business Media.
- [5] Karsten M. Borgwardt, Cheng Soon Ong, Stefan Schöner, S. V. N. Vishwanathan, Alexander J. Smola, and Hans-Peter Kriegel. 2005. Protein Function Prediction via Graph Kernels. In *Proceedings 13th International Conference on Intelligent Systems for Molecular Biology 2005, Detroit, MI, USA, 25-29 June 2005*.
- [6] Heng Chang, Yu Rong, Tingyang Xu, Wenbing Huang, Honglei Zhang, Peng Cui, Wenwu Zhu, and Junzhou Huang. 2020. A Restricted Black-Box Adversarial Framework Towards Attacking Graph Embedding Models. In *Proceedings of the 29th International Joint Conference on Artificial Intelligence, AAAI 2020*.
- [7] Jinyin Chen, Yangyang Wu, Xuanheng Xu, Yixian Chen, Haibin Zheng, and Qi Xuan. 2018. Fast Gradient Attack on Network Embedding. *arXiv:1809.02797* (2018).
- [8] Liang Chen, Jintang Li, Jiaying Peng, Tao Xie, Zengxu Cao, Kun Xu, Xiangnan He, and Z. Zheng. 2020. A Survey of Adversarial Learning on Graphs. *ArXiv* (2020).
- [9] Fan R. K. Chung. 1997. *Spectral graph theory*. American Mathematical Soc.
- [10] Michael B. Cohen, Jonathan Kelner, John Peebles, Richard Peng, Anup B. Rao, Aaron Sidford, and Adrian Vladu. 2017. Almost-Linear-Time Algorithms for Markov Chains and New Spectral Primitives for Directed Graphs. In *Proceedings of the 49th Annual ACM SIGACT Symposium on Theory of Computing, 2017 2020*.
- [11] Hanjun Dai, Hui Li, Tian Tian, Xin Huang, Lin Wang, Jun Zhu, and Le Song. 2018. Adversarial Attack on Graph Structured Data. In *Proceedings of the 35th International Conference on Machine Learning, ICML 2018, Stockholm, Sweden, July 10-15, 2018*.
- [12] Aasa Feragen, Niklas Kasenburg, Jens Petersen, Marleen de Bruijne, and Karsten M. Borgwardt. 2013. Scalable Kernels for Graphs with Continuous Attributes. In *Advances in Neural Information Processing Systems 26: 27th Annual Conference on Neural Information Processing Systems 2013. Proceedings of a Meeting Held December 5-8, 2013, Lake Tahoe, Nevada, United States*.
- [13] Justin Gilmer, Samuel S. Schoenholz, Patrick F. Riley, Oriol Vinyals, and George E. Dahl. 2017. Neural Message Passing for Quantum Chemistry. In *Proceedings of the 34th International Conference on Machine Learning, ICML 2017, Sydney, NSW, Australia, 6-11 August 2017*.
- [14] Palash Goyal and Emilio Ferrara. 2018. Graph Embedding Techniques, Applications, and Performance: A Survey. *Knowl. Based Syst.* 151 (2018).
- [15] Aditya Grover and Jure Leskovec. 2016. Node2vec: Scalable Feature Learning for Networks. In *Proceedings of the 22nd ACM SIGKDD International Conference on Knowledge Discovery and Data Mining, San Francisco, CA, USA, August 13-17, 2016*.
- [16] William L. Hamilton, Zitao Ying, and Jure Leskovec. 2017. Inductive Representation Learning on Large Graphs. In *Advances in Neural Information Processing Systems 30: Annual Conference on Neural Information Processing Systems 2017, 4-9 December 2017, Long Beach, CA, USA*.
- [17] Petter Holme and Beom Jun Kim. 2002. Growing Scale-Free Networks with Tunable Clustering. *Physical Review E* 65, 2 (2002), 026107. <https://doi.org/10.1103/PhysRevE.65.026107>
- [18] Roger A. Horn and Charles R. Johnson. 2008. *Topics in Matrix Analysis* (10. printing ed.). Cambridge Univ. Press.
- [19] Wei Jin, Yaxin Li, Han Xu, Yiqi Wang, and Jiliang Tang. 2020. Adversarial Attacks and Defenses on Graphs: A Review and Empirical Study. *ArXiv* (2020).
- [20] Thomas N. Kipf and Max Welling. 2017. Semi-Supervised Classification with Graph Convolutional Networks. In *5th International Conference on Learning Representations, ICLR 2017, Toulon, France, April 24-26, 2017, Conference Track Proceedings*.
- [21] Johannes Klicpera, Aleksandar Bojchevski, and Stephan Günnemann. 2019. Predict then Propagate: Graph Neural Networks meet Personalized PageRank. In *7th International Conference on Learning Representations, ICLR 2019, Toulon, France, 2019, Conference Track Proceedings*.
- [22] Bo Li, Yining Wang, Aarti Singh, and Yevgeniy Vorobeychik. 2016. Data Poisoning Attacks on Factorization-Based Collaborative Filtering. In *Advances in Neural Information Processing Systems 29: Annual Conference on Neural Information Processing Systems 2016, December 5-10, 2016, Barcelona, Spain*.
- [23] Qimai Li, Zhichao Han, Yuriy Wu, and Xiao-Ming. 2018. Deeper Insights into Graph Convolutional Networks for Semi-supervised Learning. In *Proceedings of the 27th International Joint Conference on Artificial Intelligence, AAAI 2018*.
- [24] László Lovász et al. 1993. Random walks on graphs: A survey. *Combinatorics, Paul erdos is eighty 2*, 1 (1993), 1–46.
- [25] Hoang NT and Takanori Maehara. 2019. Revisiting Graph Neural Networks: All We Have is Low-Pass Filters. *arXiv:1905.09550 [cs, math, stat]* (2019).
- [26] Ashwin Paranjape, Austin R. Benson, and Jure Leskovec. 2017. Motifs in Temporal Networks. In *Proceedings of the 10th ACM International Conference on Web Search and Data Mining, WSDM 2017, Cambridge, United Kingdom, February 6-10, 2017*.
- [27] Bryan Perozzi, Rami Al-Rfou, and Steven Skiena. 2014. DeepWalk: Online Learning of Social Representations. In *Proceedings of 20th ACM SIGKDD International Conference on Knowledge Discovery and Data Mining, KDD '14, New York, NY, USA - August 24 - 27, 2014*.
- [28] Prithviraj Sen, Galileo Namata, Mustafa Bilgic, Lise Getoor, Brian Galligher, and Tina Eliassi-Rad. 2008. Collective Classification in Network Data. *AI Magazine* 29, 3 (2008).
- [29] Daniel A. Spielman and Shang-Hua Teng. 2008. Spectral Sparsification of Graphs. *SIAM J. Comput.* (2008).
- [30] G. W. Stewart and Ji-guang Sun. 1990. *Matrix Perturbation Theory*. Academic Press, Boston.
- [31] Binghui Wang and Neil Zhenqiang Gong. 2019. Attacking Graph-Based Classification via Manipulating the Graph Structure. In *Proceedings of the 2019 ACM SIGSAC Conference on Computer and Communications Security, CCS 2019, London, UK, November 11-15, 2019*.
- [32] Hongwei Wang, Fuzheng Zhang, Mengdi Zhang, Jure Leskovec, Miao Zhao, Wenjie Li, and Zhongyuan Wang. 2019. Knowledge-Aware Graph Neural Networks with Label Smoothness Regularization for Recommender Systems. In *Proceedings of the 25th ACM SIGKDD International Conference on Knowledge Discovery and Data Mining, KDD 2019, Anchorage, AK, USA, August 4-8, 2019*.
- [33] Xiaoyun Wang, Joe Eaton, Cho-Jui Hsieh, and Shytsun Felix Wu. 2018. Attack Graph Convolutional Networks by Adding Fake Nodes. *ArXiv* (2018).
- [34] Duncan J. Watts and Steven H. Strogatz. 1998. Collective Dynamics of ‘Small-World’ Networks. *Nature* 393, 6684 (1998), 440–442. <https://doi.org/10.1038/39018>
- [35] Felix Wu, Amauri H. Souza Jr, Tianyi Zhang, Christopher Fifty, Tao Yu, and Kilian Q. Weinberger. 2019. Simplifying Graph Convolutional Networks. In *Proceedings of the 36th International Conference on Machine Learning, ICML 2019, 9-15 June 2019, Long Beach, California, USA*.
- [36] Huijun Wu, Chen Wang, Yuriy Tyshetskiy, Andrew Docherty, Kai Lu, and Liming Zhu. 2019. Adversarial Examples for Graph Data: Deep Insights into Attack and Defense. In *Proceedings of the 28th International Joint Conference on Artificial Intelligence, IJCAI 2019, Macao, China, August 10-16, 2019*.
- [37] Kaidi Xu, Hongge Chen, Sijia Liu, Pin-Yu Chen, Tsui-Wei Weng, Mingyi Hong, and Xue Lin. 2019. Topology Attack and Defense for Graph Neural Networks: An Optimization Perspective. In *Proceedings of the 28th International Joint Conference on Artificial Intelligence, IJCAI 2019, Macao, China, August 10-16, 2019*.
- [38] Keyulu Xu, Weihua Hu, Jure Leskovec, and Stefanie Jegelka. 2019. How Powerful Are Graph Neural Networks?. In *7th International Conference on Learning Representations, ICLR 2019, New Orleans, LA, USA, May 6-9, 2019, OpenReview.net*.
- [39] Qi Xuan, Jun Zheng, Lihong Chen, Shanjing Yu, Jinyin Chen, Dan Zhang, and Qingpeng Zhang. 2019. Unsupervised Euclidean Distance Attack on Network Embedding. *ArXiv* (2019).
- [40] Zitao Ying, Jiaxuan You, Christopher Morris, Xiang Ren, William L. Hamilton, and Jure Leskovec. 2018. Hierarchical Graph Representation Learning with Differentiable Pooling. In *Advances in Neural Information Processing Systems 31: Annual Conference on Neural Information Processing Systems 2018, NeurIPS 2018, 3-8 December 2018, Montréal, Canada*.
- [41] Dingyuan Zhu, Ziwei Zhang, Peng Cui, and Wenwu Zhu. 2019. Robust graph convolutional networks against adversarial attacks. In *Proceedings of the 25th*

ACM SIGKDD International Conference on Knowledge Discovery and Data Mining, KDD 2019, Anchorage, AK, USA, August 4-8, 2019.

- [42] Xiaojin Zhu and Zoubin Ghahramani. 2003. *Learning from Labeled and Unlabeled Data with Label Propagation*. Technical Report. Carnegie Mellon University.
- [43] Daniel Zügner, Amir Akbarnejad, and Stephan Günnemann. 2018. Adversarial Attacks on Neural Networks for Graph Data. In *Proceedings of the 24th ACM SIGKDD International Conference on Knowledge Discovery and Data Mining, KDD 2018, London, UK, August 19-23, 2018*.
- [44] Daniel Zügner and Stephan Günnemann. 2019. Adversarial Attacks on Graph Neural Networks via Meta Learning. In *7th International Conference on Learning Representations, ICLR 2019, New Orleans, LA, USA, May 6-9, 2019*.

## A APPENDIX

### A.1 Additional theorems

**THEOREM 4.** (*Wely’s inequality for singular values [18]*). *Let two symmetric matrices  $P, Q \in \mathbb{R}^{N \times N}$ . Then, for the decreasingly ordered singular values  $\sigma$  of  $P, Q$  and  $PQ$ , we have  $\sigma_{i+j-1}(PQ) \leq \sigma_i(Q) \times \sigma_j(P)$  for any  $1 \leq i, j \leq N$  and  $i + j \leq N + 1$ .*

### A.2 Notations

The main notations can be found in the Table 7.

**Table 7: Definition of major symbols.**

Notation	Description
$G, A, S, E$	The original graph, the adjacency matrix, the generic graph filter and the edge set of $G$
$G', A', S', E'$	The perturbed graph, the adjacency matrix, the generic graph filter and the edge set of $G'$
$u, u'$	The generalized eigenvectors of $A$ and $A'$
$\lambda, \lambda'$	The generalized eigenvalues of $A$ and $A'$
$\lambda(A), \lambda(A')$	The eigenvalues of $A$ and $A'$
$\lambda(S), \lambda(S')$	The eigenvalues of $S$ and $S'$
$\alpha$	The normalization parameter of the generic graph filter $S$
$\delta$	The perturbation budget
$k$	The spatial coefficient
$\theta$	The restart threshold
$r$	The number of restart
$\epsilon$	The approximation error of the perturbed eigenvectors

### A.3 Additional results

**Can heuristics explain adversarial edges?** A most straightforward strategy of identifying adversarial edges is to utilize simple heuristics to capture “important” edges [3]. However, recall that in Table 1, some results unexpectedly revealed that some heuristic methods (*i.e.*, *Deg.*, *Betw.*, *Eigen.*) sometimes performs worse than randomly selection of adversarial edges. We heres analyze this observation by comparing the degree, betweenness or eigenvector centrality distribution of our selected adversarial edges with that of the randomly selected edges. In Figure 5, we find that our selected adversarial edges tend to have smaller degree, betweenness or eigenvector centrality. Whereas, common heuristic methods, following a previous work [3], are performed by selecting the adversarial edges with bigger centrality (indicating their importance). Our findings actually run counter to these heuristic methods, thus this is one possible reason why they perform badly. Moreover, Eq. 4 gives us an intuitive spectral view to analyze the degree centrality, *i.e.*, the spectrum of  $S'$  is upper bounded by a term w.r.t the smallest degree in  $G'$ .

We therefore propose to select adversarial edges based on the increasing order of the sum of the degree/betweenness/eigenvector centrality (*i.e.*, *SmallDeg.*, *SmallBetw.* and *SmallEigen.*) and report

their results as the setting of node-level attack in Table 8. We observe that the smaller centrality does perform better than the larger one in most cases although still can not beat our method.

**Table 8: The relative decrease in Macro-F1 score of additional heuristic methods with standard deviation of node-level attacks against three types of victim models.**

		<i>SmallDeg.</i>	<i>SmallBetw.</i>	<i>SmallEigen.</i>
Cora-ML	GCN	$2.27 \pm 0.4$	$2.29 \pm 0.6$	$1.44 \pm 0.4$
	node2vec	$4.47 \pm 0.9$	$5.64 \pm 1.4$	$4.85 \pm 0.8$
	Label Prop.	$5.14 \pm 0.6$	$5.37 \pm 0.5$	$4.63 \pm 0.3$
Citeseer	GCN	$2.77 \pm 0.7$	$2.81 \pm 0.6$	$2.34 \pm 0.8$
	node2vec	$5.78 \pm 2.4$	$7.99 \pm 2.0$	$2.26 \pm 1.7$
	Label Prop.	$7.66 \pm 0.8$	$7.53 \pm 1.3$	$5.33 \pm 0.5$
Polblogs	GCN	$3.14 \pm 0.8$	$2.64 \pm 1.0$	$3.58 \pm 0.7$
	node2vec	$2.00 \pm 0.5$	$1.33 \pm 0.6$	$1.75 \pm 0.7$
	Label Prop.	$4.81 \pm 0.6$	$4.71 \pm 0.7$	$5.92 \pm 0.8$

**The selection of candidate set.** We have mentioned that one limitation of our attack strategy is the randomly selected candidate set, which introduces a further approximation. We here further analyze the impact of the candidate set size. Figure 6 shows the relative decrease when we choose the size of candidate set among {10k, 20k, 30k, 40k, 50k}. We observe that although our model performs slightly better if we randomly select 50k edge pairs as the candidate, the candidate size appears to have little influence on the overall performance, which partly verifies the practical utility of our strategy of randomly selecting candidates.

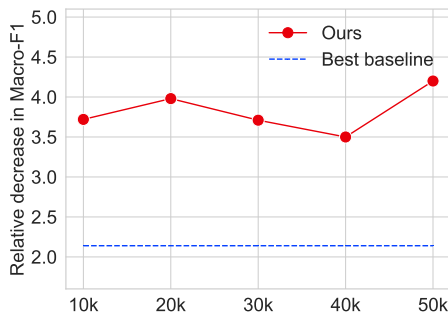


**Figure 6: The relative decrease in Macro-F1 score of node-level attacks against GCN with different size of the candidate set on Citeseer dataset. The blue dashed line denotes the performance of the best baseline when candidate size is chosen as 20k.**

**Detailed results of Table 1.** We further report the detailed results (decrease in Macro-F1 score, Macro-Precision score and Macro-Recall score) with standard deviation of node-level attacks in Table 9.

**Parameter Analysis.** Our algorithm involves two hyperparameters: namely, the spatial coefficient  $k$  and restart threshold  $\theta$ . We use grid search to find their suitable values on Cora-ML and present here for reference (see Figure 7). Better performance can be obtained when  $k \in \{1, 2\}$  and  $\theta \leq 0.03$ . The observation that our model’s superiority when  $k \leq 2$  is consistent with many conclusions of over-smoothing problem on graphs [21, 23]. Remarkably, our model can still achieve relatively good performance (*i.e.*, better than the baseline methods) regardless of how these parameters are changed.

#### A.4 Dataset details

**Synthetic datasets.** We use four synthetic random graphs to evaluate the approximation quality. For the Erdős–Rényi graph, we set the probability for edge creation as 0.01. For the Barabási–Albert graph, we set the number of edges attached from a new node to existing nodes as 5. When generating the Watts–Strogatz graph, each node is connected to its 10 nearest neighbors in a ring topology, and the probability of rewiring each edge is 0.1. When generating growing graphs with the powerlaw degree distribution [17], the number of random edges to add for each new node is 5, and the probability of adding a triangle after adding a random edge is 0.1.

**Real-world datasets.** We use three social network datasets: Cora-ML, Citeseer and Polblogs. The former two are citation networks mainly containing machine learning papers. Here, nodes are documents, while edges are the citation links between two documents. Each node has a human-annotated topic as the class label as well as a feature vector. The feature vector is a sparse bag-of-words representation of the document. All nodes are labeled to enable differentiation between their topic categories. Polblogs is a network of weblogs on the subject of US politics. Links between blogs are extracted from crawls of the blog’s homepage. The blogs are labelled to identify their political persuasion (liberal or conservative). Detailed statistics of the social network datasets are listed in Table 10.

We also use two protein graph datasets: Proteins and Enzymes. Proteins is a dataset in which nodes represent secondary structure elements (SSEs) and two nodes are connected by an edge if they are neighbors in either the amino-acid sequence or 3D space. The label indicates whether or not a protein is a non-enzyme. Moreover, Enzymes is a dataset of protein tertiary structures. The task is to correctly assign each enzyme to one of the six EC top-level classes. More detailed statistics of the protein graph datasets are listed in Table 11.

#### A.5 Implementation Details

Here, we provide additional implementation details of our experiments in § 4.

For GCN, GIN and Diffpool, we use PyTorch Geometric<sup>1</sup> for implementation. We set the learning rate as 0.01 and adopt Adam as our optimizer. For Node2vec, we use its default hyper-parameter setting [15], but set the embedding dimension to 64 and use the implementation by CogDL<sup>2</sup>. A logistic regression classifier is then

<sup>1</sup>[https://github.com/rusty1s/pytorch\\_geometric](https://github.com/rusty1s/pytorch_geometric)

<sup>2</sup><https://github.com/THUDM/cogdl>

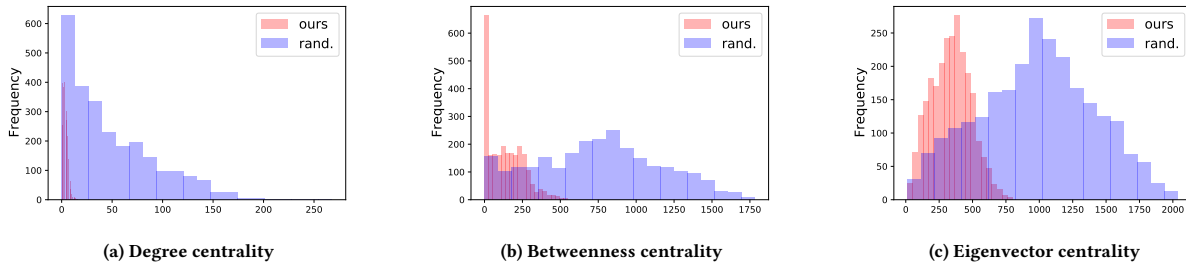


Figure 5: The comparison of the centrality distributions for our selected adversarial edges and those of the randomly selected edges on Polblogs dataset.

Table 9: The detailed experimental results with standard deviation of node-level attacks against three types of victim models. We report the decrease of performance (in percent) on the test set after the attack is performed; the higher the better (note that negative results denote that the performance adversely increases after the attack). We also report the performance on the unattacked graph.

		(Unattacked)	Rand.	Deg.	Betw.	Eigen.	DW	GPGD	Ours-r	Ours	White-box	
Cora-ML	GCN	F1	0.82±0.8	1.97±0.8	1.12±0.4	1.22±0.4	0.28±0.3	0.85±0.3	4.22±0.6	5.02±0.4	<b>5.27±0.3</b>	11.36±0.5
		Prec.	0.81±0.9	0.55±0.5	0.20±0.4	0.11±0.3	0.18±0.3	0.32±0.2	1.69±0.6	3.02±0.4	<b>3.43±0.3</b>	6.58±0.6
		Recall	0.82±1.1	1.15±0.9	0.94±0.4	1.23±0.6	0.49±0.4	0.87±0.4	2.51±0.6	3.84±0.4	<b>4.05±0.4</b>	6.87±0.4
	Node2vec	F1	0.79±0.8	6.37±1.8	5.40±1.6	3.33±1.0	2.84±1.0	3.25±1.3	5.33±1.8	6.92±1.0	<b>8.29±1.0</b>	1.43±0.9
		Prec.	0.78±0.7	6.06±1.8	3.04±1.7	3.64±0.9	2.15±1.1	2.96±1.3	4.96±1.7	5.95±1.0	<b>8.04±1.0</b>	1.39±1.0
		Recall	0.78±0.9	6.69±2.0	3.76±1.5	4.92±1.3	3.01±1.0	3.57±1.4	5.10±1.8	6.32±1.0	<b>8.54±0.9</b>	1.52±1.1
Label Prop.	F1	0.80±0.7	4.10±1.3	2.45±0.7	2.71±0.8	2.07±0.7	1.79±0.9	4.28±1.6	6.02±0.9	<b>7.13±0.9</b>	1.05±1.0	
	Prec.	0.81±0.8	2.98±1.3	1.10±0.6	1.20±0.4	1.46±0.7	1.05±0.8	3.05±1.0	4.62±0.8	<b>4.98±1.0</b>	0.09±0.8	
	Recall	0.80±1.0	4.95±1.2	3.61±0.9	4.32±1.0	2.64±0.9	2.54±1.2	5.03±1.9	7.92±1.0	<b>7.99±1.0</b>	1.51±1.0	
Citeseer	GCN	F1	0.66±1.4	2.02±0.6	0.16±0.4	0.70±0.4	0.64±0.4	0.21±0.4	2.14±0.9	3.16±0.6	<b>3.98±0.5</b>	6.42±0.6
		Prec.	0.64±1.6	1.15±0.7	0.10±0.5	0.33±0.2	0.30±0.4	0.09±0.5	2.01±0.8	2.94±0.6	<b>3.28±0.7</b>	5.92±0.6
		Recall	0.64±1.6	1.90±0.6	-81.41±245.3	0.72±0.4	0.64±0.5	0.13±0.4	2.51±0.9	3.62±0.7	<b>4.00±0.5</b>	7.06±0.5
	Node2vec	F1	0.60±1.5	7.47±2.3	7.47±1.6	3.47±2.6	4.87±1.5	2.54±2.5	5.26±1.9	8.32±2.5	<b>9.32±2.6</b>	0.12±1.0
		Prec.	0.59±1.6	7.28±2.4	7.33±2.1	3.01±2.7	4.26±1.5	2.88±3.2	5.00±1.9	7.91±2.4	<b>8.69±2.7</b>	0.10±1.0
		Recall	0.62±1.5	7.24±2.2	6.94±1.6	4.51±2.4	5.00±1.4	2.62±2.5	5.86±1.9	8.69±2.5	<b>9.86±2.7</b>	0.19±1.0
Label Prop.	F1	0.64±0.8	7.12±1.3	3.47±0.8	6.00±1.7	5.36±0.6	3.00±0.8	5.14±1.9	7.79±0.9	<b>8.16±0.9</b>	2.47±1.2	
	Prec.	0.62±0.8	6.35±1.5	2.95±0.6	5.59±1.8	5.06±0.6	2.54±0.6	4.52±1.8	6.69±1.0	<b>7.77±0.9</b>	2.06±1.1	
	Recall	0.67±0.7	7.50±1.2	3.01±0.9	4.35±1.8	6.02±0.6	3.10±0.9	5.45±1.9	8.16±0.9	<b>8.55±1.0</b>	2.66±1.2	
Polblogs	GCN	F1	0.96±0.7	1.91±1.5	0.03±0.2	1.72±0.6	0.67±0.5	0.01±0.4	2.35±1.8	4.30±1.2	<b>5.32±1.1</b>	3.88±1.1
		Prec.	0.95±0.7	1.65±1.0	0.02±0.2	1.51±0.5	0.35±0.5	0.02±0.3	2.10±1.8	4.02±1.1	<b>4.99±1.0</b>	3.05±1.0
		Recall	0.96±0.7	1.93±1.5	0.01±0.1	1.74±0.6	0.75±0.5	0.01±0.4	2.53±1.9	4.58±1.2	<b>6.01±1.0</b>	4.06±1.1
	Node2vec	F1	0.95±0.3	3.01±0.7	0.04±0.6	3.07±0.6	1.84±0.3	0.18±0.4	2.49±0.6	2.74±0.5	<b>3.79±0.5</b>	2.13±0.4
		Prec.	0.95±0.3	2.01±0.6	0.03±0.5	3.06±0.6	1.22±0.4	0.17±0.5	2.06±0.7	2.65±0.5	<b>3.51±0.4</b>	2.09±0.4
		Recall	0.95±0.3	3.04±0.7	0.04±0.4	3.04±0.6	2.66±0.3	0.18±0.8	2.66±0.5	2.94±0.5	<b>3.99±0.5</b>	2.13±0.3
Label Prop.	F1	0.96±0.5	4.99±0.7	0.08±0.4	3.45±0.7	2.15±0.3	0.37±0.5	4.15±0.8	5.84±0.7	<b>6.14±0.7</b>	2.28±0.5	
	Prec.	0.96±0.5	4.41±0.8	0.10±0.4	3.03±0.6	2.45±0.8	0.34±0.4	3.51±0.7	5.05±0.8	<b>5.08±0.7</b>	2.05±0.5	
	Recall	0.96±0.5	4.67±0.8	0.04±0.4	3.15±0.7	2.05±0.8	-87.62±264.2	4.22±0.8	5.86±0.7	<b>6.56±0.6</b>	2.51±0.5	

used for classification given the embedding. For Label Propagation, we use an implementation that is adapted to graph-structured data<sup>3</sup>.

For all target models, we tune the number of epochs based on convergence performance. When performing GCN on Cora-ML, Citeseer and Polblogs, the number of epochs is set to 100. When performing GIN or Diffpool on Enzymes, we set the number of epochs to 20, while when performing GIN on Proteins, the number

<sup>3</sup><https://github.com/thibaudmartinez/label-propagation>

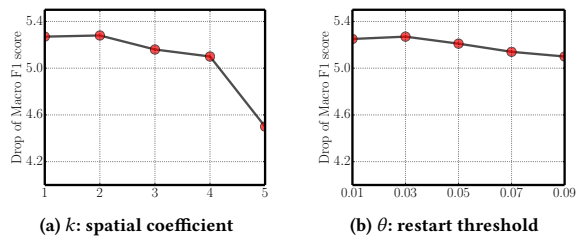


Figure 7: Parameter analysis for node classification task.

Table 10: Data statistics of social datasets

dataset	Cora-ML	Citeseer	Polblogs
<b>type</b>	citation network	citation network	web network
<b># vertices</b>	2,810	2,110	1,222
<b># edges</b>	7,981	3,757	16,714
<b># classes</b>	7	6	2
<b># features</b>	1,433	3,703	0

Table 11: Data statistics of protein datasets

dataset	Proteins	Enzymes
<b>type</b>	protein network	protein network
<b># graphs</b>	1,113	600
<b># classes</b>	2	6
<b># features</b>	3	3
<b>avg # nodes</b>	39.06	32.63
<b>avg # edges</b>	72.82	62.14

of epochs is set to 10. Finally, when performing Diffpool on Proteins, the number of epochs is set to 2. All experiments are conducted on a single machine with an Intel Xeon E5 and a NVIDIA TITAN GPU.

When implementing baselines, we directly apply the default hyperparameters of *DW* [3], another black-box attack [6] and *Nettack* [43]. For *GPGD* [37] adopting  $\ell_1(A')$  as the objective, we train 500 epochs with a decaying learning rate as  $lr = lr\_init / (1 + i * decay\_rate)$  where  $lr\_init$  is the initial learning rate,  $decay\_rate$  is the decaying rate and  $i$  is the current number of iterations. We set the initial learning rate as  $2e-4$  with a decaying rate 0.2 on Cora-ML, set the initial learning rate  $1e-3$  as with a decaying rate 0.2 on Citeseer, Polblogs, and set the initial learning rate  $1e-2$  as with a decaying rate 0.2 on Proteins and Enzymes. When applying *GPGD* for the white-box setting, we set the learning rate as 10 and run 700 epochs.